A dual-beam photothermal reflection based system for thermal diffusivity measurement of optically dense liquids

Blanca Jaimes, Dervin Pulgar, María Antonieta Ranaudo, José Chirinos, and Manuel Caetano[a)]
Facultad de Ciencias, Escuela de Química, Universidad Central de Venezuela, P.O. Box 40720, 1041A Caracas, Venezuela

(Received 15 September 2009; accepted 2 January 2010; published online 5 February 2010)

A dual-beam photothermal reflection based system capable to measure thermal diffusivities of optically dense liquids has been designed and implemented. The large optical absorption coefficient of these liquids inhibits the possibility to use conventional transmission instruments for direct thermal diffusivity measurements. To overcome this problem, a front heating front detection photothermal reflection system has been proposed. This method expands the range of application and simplifies the experimental procedure of traditional photothermal methods, allowing precise measurement of thermal diffusivity of a variety of liquids. Measurements of the change in thermal diffusivity with the concentration of asphaltene in toluene solutions are described to test the applicability of this technique for reliable measurements of thermal diffusivities of optically dense liquids. © *2010 American Institute of Physics.* [doi:10.1063/1.3297900]

I. INTRODUCTION

Thermal diffusivity of a material (α) is a very important physical property associated with transient heat flow. It measures the ability of a material to conduct thermal energy relative to its ability to store thermal energy. It is related to thermal conductivity k_T, specific heat C_p, and density ρ,[1]

$$\alpha = \frac{k_T}{C_p \rho}. \tag{1}$$

According to the above equation, thermal diffusivity can be calculated indirectly from the measured thermal conductivity, density, and specific heat. However, this approach needs considerable time and different instrumentation.

Photothermal methods have been used to monitor the thermal state of the analytical samples.[2–7] These methods are based on monitoring the changes in the refractive index changes associated with effects generated by deposition of heat in a sample, due to nonradiative de-excitation following absorption of radiation. All these methods are simple, versatile, accurate, noncontact, and thus nondestructive approach methods, being exceedingly appropriate for the measurement of thermal properties of materials.

Photothermal methods based on sample reflection changes have been used extensively in several areas of science and technology, particularly for studies of the thermal conductivity of thin films,[8,9] the thermal conductance of interfaces,[10] and thermal diffusivity of solids.[11,12] In general, an increase of the temperature in the solid causes a broadening and shift of the absorption edges. Through the Kramers–Kronig relation, this produces a change in the refraction index of the material and thus there is a temperature dependence of the reflection coefficient.

Comeau *et al.*,[13] using a pump-probe laser technique, were able to generate changes in the reflectance on thin chromium and beryllium films deposited on glass substrates. They call the spatial distribution of the refraction index generated at the surface of the film a "reflected thermal lens." The dynamics of the thermal lens is found to be closely related to the thermal properties of its environment when the film is in contact with a liquid and the film is periodically heated with an optical source. This dependence was used to obtain the thermal diffusivity of a variety of liquids placed in contact with the film. Reflected thermal lens can be applied to opaque liquids and this is the main advantage over transmission lens spectroscopy.

In this article, we present a simple, noncontact, dual-beam system, based on the studies of Comeau *et al.*,[13] to follow changes in the thermal diffusivity of opaque liquid systems, even in closed systems, without disturbing the sample. The aligning and coupling of the two beams were easily accomplished by using a Dove prism.

II. INSTRUMENTAL ARRANGEMENTS

Figure 1 presents a schematic representation of the photothermal reflection spectrometer. It consisted of a 15 mW air-cooled argon-ion laser (Spectra Physics 161B-514) at 514.5 nm, as the excitation source, and a 5 mW He–Ne laser (CVI-Melles Griot 05-LHR) as the probe beam. The two laser beams were coupled in a front heating, front detection (FF) type of configuration by using a Dove prism ($2.54 \times 2.54 \times 10.2$ cm^3) from CVI-Mellets Griot, with antireflection coatings on the ends. The advantages of FF over other configurations are (i) large reflectance signal and (ii) applicable to films on opaque solutions, which is precisely our

[a)]Author to whom correspondence should be addressed. Electronic mail: manuel.caetano@ciens.ucv.ve.

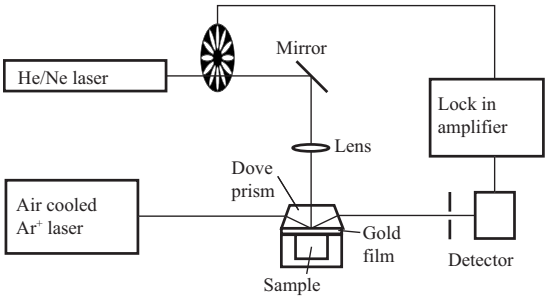

FIG. 1. Schematic diagram of the experimental assembly.

case. A thin gold film (~100 nm) sputtered over the hypotenuse side of the prism worked as a reflective surface. The prism was previously soaked for 45 min at 90 °C in a mixture of freshly prepared 3:1 concentrate sulfuric acid to 30% hydrogen peroxide (piranha solution) to assure a better adherent surface to the gold film. UV-visible absorption spectrum of a 100 nm thick gold film deposited on a 1 mm thick glass substrate (microscope slide) is shown in Fig. 2. The excitation beam, which was amplitude modulated by a mechanical chopper, was normally directed along the hypotenuse face of the prism. The excitation beam was focused onto the gold film surface by using a planoconvex spherical lens, L_1 (200 mm focal length). The probe beam enters through one of the sloped faces of the prism and is parallel to hypotenuse face, undergoes reflection at the metal film, and emerges from the opposite sloped face parallel to its incident direction.

The optical setup allows for a mode-mismatched condition at the metal film, where the excitation beam diameter is smaller than the probe beam diameter. The relative size of the excitation and probe beams m was 80/120.

The sample cell consists of a round aluminum bar (40 mm of diameter and 50 mm long) with a central bore, closed at one end, parallel to its long side. Perpendicular to this bore, one hole completes a liquid container with in- and outlet openings. The open end of the concentric bore is pressed against the prism hypotenuse, allowing direct contact between liquid samples and the gold film. An O-ring in between provides liquid tightness. The sample cell is held in place by four screws. Figure 3 shows a cross section of the sample cell and Dove prism assembled.

The time-dependent signal was obtained by sampling the

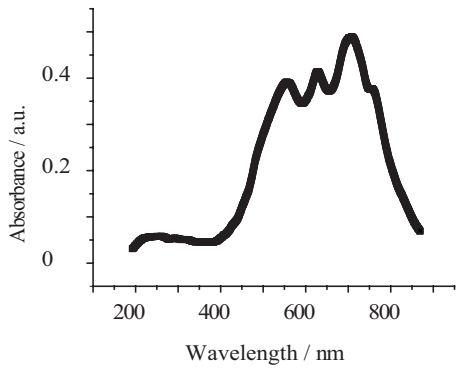

FIG. 2. UV-visible absorption spectra of a 100 nm thick gold film deposited on a 1 mm thick glass substrate.

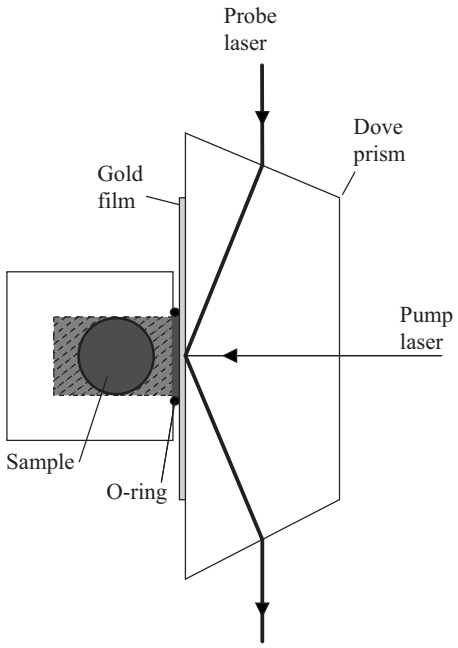

FIG. 3. Dove prism and sample stage assembled.

intensity at the center of the reflected probe beam through a precision pinhole (100 mm), with a PIN silicon photodiode (Melles Griot LM2). The pinhole and the detector were jointly mounted in a laboratory made device held on an *X-Y-Z* translator, in order to localize the center of the laser beam. The photodiode current, converted in voltage, was amplified by a low-noise preamplifier (Melles Griot 13-AMP-003) and fed into a lock-in amplifier (SR830) using a reference signal generated by the chopper. The chopped cw laser excitation and lock-in detection displayed a signal that was proportional to the full peak-to-peak periodical signal, that is, to the difference between the intensities of the reflected probe beam at the start and at the end of the pump irradiation (an "on" period of the chopper cycle).[2,14]

Figure 4 shows intensity profiles of the reflected probe beam with (a) no pump present and (b) 35 mW pumping power and $m=80/120$. The profiles were constructed by tak-

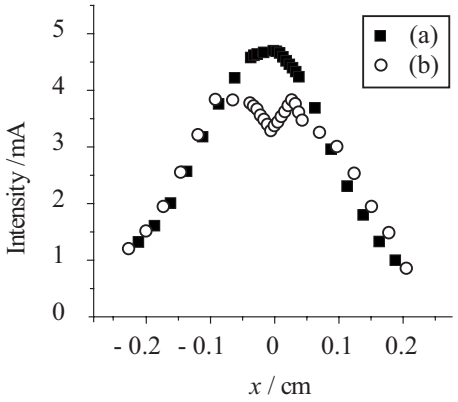

FIG. 4. Profile of the reflected probe beam with (a) no pump present and (b) 35 mW pumping power and beam size ratio (pump over probe) $m=80/120$.

TABLE I. Properties of liquids used in the calibration procedure (ρ: density; C_p: heat capacity; k: electric conductivity; α: thermal diffusivity).

Liquids	ρ (g cm^{-3})	C_p (J g^{-1} K^{-1})	k (W m K^{-1})	$\alpha\times10^{-8}$ (m^{-2} s^{-1})
Propan-2-ol[a]	0.786	2.60	0.135	6.60
Propan-1-ol[a]	0.804	2.39	0.154	8.00
Ethanol[b]	0.982	1.68	0.165	10.02
Propan-2-one[b]	0.79	2.17	0.161	9.37
Methanol[c]	0.791	2.53	0.200	9.98
Methyl cyanide[d]	0.786	2.23	0.188	10.75
Water	0.997	4.18	0.598	14.31
Ethyl acetate	0.902	1.94	0.144	8.26
Chloroform[c]	1.483	0.96	0.117	8.25
Heptane[c]	0.684	2.24	0.123	8.01
Toluene[b]	0.867	1.71	0.131	8.86
Carbon tetrachloride[e]	1.594	0.85	0.099	7.31
Benzene[f]	0.879	1.71	0.137	9.11

[a]Fluka.
[b]Riedel–de Haën.
[c]Burdick & Jackson.
[d]EM Science.
[e]Merck.
[f]Hopkin & Williams.

ing sample sections of the beam by moving a precision pin hole (50 μm) through the beam and detecting the intensity with a modified webcam (genius express).

III. RESULTS AND DISCUSSION

A. Calibration of the system

The absorbed heat is dissipated away from the film into the liquid in a more effective way than laterally into the film because of the greater area of exposure and temperature gradient.[13] Hence, both the heat dissipation rate and, in consequence, the full peak-to-peak periodical signal from the reflection of the probe beam should depend on the thermal diffusivity of the liquid in contact with the film. Because of this dependence, the thermal diffusivity of liquids can be measured indirectly in the photothermal reflection instrument.[13]

In order to obtain photothermal data, which can be quantitatively related to the amount of energy absorbed and the amount of energy released nonradiatively, a calibration of the experimental setup is required.

The calibration was carried out over a suitable range of diffusivities values by taking measurements with the film in contact with each one of a set of organic and inorganic liquids listed in Table I. Probe reflected signal at a constant modulation frequency from the excitation laser, as a function of the thermal diffusivity, is reported in Fig. 5. Measurements were taken with powers of 35 and 5 mW for the excitation and probe beams, respectively, and a chopper frequency of 15 Hz. An empirical model, represented by a second order polynomial expression, was fitted by least-squares to the data, yielding the equation

$$\hat{y} = 1.68 + 0.22x - 0.017x^2, \tag{2}$$

which is also plotted as a solid curve in Fig. 5. The R-squared statistic indicates that the model as fitted explains

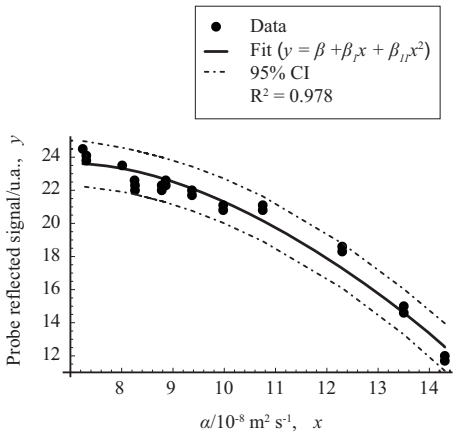

FIG. 5. Probe reflected signal as a function of the thermal diffusivity of the liquids. A quadratic model was fitted to the data (solid curve), and a 95% confidence two sided band for it is displayed (dashed lines).

97.8 % of the variability in α. Scatter plots of the residuals versus thermal diffusivity and versus predicted values do not exhibit any systematic structure, indicating that the model fits the data well.

To validate the quadratic model, thermal diffusivities of different liquids, not employed in the calibration procedure, were experimentally estimated using Eq. (2) as a calibration curve, and compared against the theoretical predictions (Table II).

B. Phase change in asphaltene solutions followed by changes in thermal diffusivity

The applicability of the new instrument to optically dense solutions was verified by means of a study of phase change of asphaltene in toluene solutions. In aromatic solvents, such as toluene, asphaltenes have a tendency to form aggregates whose structure and formation still remains unknown despite much research.[15] Asphaltene aggregates seem to have a maximum size limit in the order of nanometers, and can be treated as entities with a reasonably well-defined density and compressibility.[16] Polydispersity, chemical composition, and steric arrangement or interconnectivity of functional groups in the asphaltenes monomers, stabilize these "nanoaggregates," which are suspended by Brownian motion. Asphaltenes aggregation is accompanied by a change in thermal diffusivity enabling this optical technique to determine concentration of asphaltenes aggregates formation.

Asphaltenes were obtained from crude oil as described earlier.[17] Extraheavy Cerro Negro crude oil was diluted with

TABLE II. Comparison of the thermal diffusivity theoretically predicted with the experimental estimate for various organic liquids.

	$\alpha\times10^{-8}$/m^{-2} s^{-1}	
Solvents	Theoretical	Experimental
n-pentane	7.79	7.3 ± 0.1
n-hexane	8.07	7.8 ± 0.1
n-decane	8.18	8.0 ± 0.1
Cyclohexane	8.58	8.6 ± 0.2
Carbon disulfide	11.73	11.5 ± 0.2

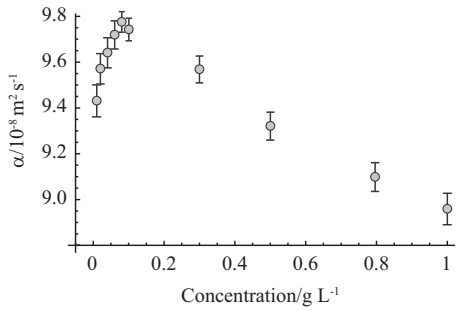

FIG. 6. Thermal diffusivities (α) vs asphaltene in toluene concentration. An inverted V-shaped curve can be associated with two different stages in asphaltenes aggregation.

toluene [1:1 (v/v)] before the addition of *n*-heptane (40 v). Precipitated resins were removed by Soxhlet extraction with boiling *n*-heptane. Solutions ranging from 0.01 to 1 g l^{-1} were prepared by dilution and experiments were performed after a three-day period to minimize aging problems. The sample cell was filled with 2 mL of solution, and enough time was allowed for the solutions to reach thermal equilibrium and chemical stability before any measurement was made. The measurement consisted in the full peak-to-peak periodical signals observed in the lock-in amplifier from the reflection of the probe beam. The thermal diffusivity was estimated by using Eq. (2) as a calibration curve.

Figure 6 describes the variations of thermal diffusivities versus asphaltenes concentration in toluene solution. These thermal diffusivities yield an inverted V-shaped curve with a maximum point at 0.1 g l^{-1}. This behavior indicates a crossover between two different regimes of heat diffusion that can be related with changes in the distribution and/or association of the asphaltenes aggregation starting at 0.1 g l^{-1}, and they are in agreement with Refs. 15 and 18.

IV. CONCLUSION

In conclusion, we have presented an extremely simple and easy to use system; consisting in a dual beam, front heating-front detection, thermoreflectance assembly. The experimental results demonstrated that this system design could be used effectively to measure the thermal diffusivities of various liquids, even optically dense samples.

ACKNOWLEDGMENTS

This work was supported by grants from FONACIT (Grant Nos. G-2005000430 and S1-2001000877) and CDCH-UCV (Grant No. G-03-00-65467-2006/1).

[1] Y. Touloukian, *Thermal Diffusivity* (IFI/Plenum, New York, 1973).
[2] S. Bialkowski, *Photothermal Spectroscopy Methods for Chemical Analysis* (Wiley-Interscience, New York, 1996).
[3] A. C. Tam, Rev. Mod. Phys. **58**, 381 (1986).
[4] M. J. Adams, J. G. Highfield, and G. F. Kirkbright, Anal. Chem. **49**, 1850 (1977).
[5] J. Shen, R. D. Lowe, and R. D. Snook, Chem. Phys. **165**, 385 (1992).
[6] H. Vargas and L. C. Miranda, Rev. Sci. Instrum. **74**, 794 (2003).
[7] M. P. P. Castro, A. A. Andrade, R. W. A. Franco, P. C. M. L. Miranda, M. Sthel, H. Vargas, R. Constantino, and M. L. Baesso, Chem. Phys. Lett. **411**, 18 (2005).
[8] R. M. Costescu, M. A. Wall, and D. G. Cahill, Phys. Rev. B **67**, 054302 (2003).
[9] R. M. Costescu, A. J. Bullen, G. Matamis, K. E. O. Hara, and D. G. Cahill, Phys. Rev. B **65**, 094205 (2002).
[10] S. Huxtable, D. G. Cahill, V. Fauconnier, J. O. White, and J.-C. Zhao, Nat. Mater. **3**, 298 (2004).
[11] N. Taketoshi, T. Baba, and A. Ono, Meas. Sci. Technol. **12**, 2064 (2001).
[12] K. Hatori, N. Taketoshi, T. Baba, and H. Ohta, Rev. Sci. Instrum. **76**, 114901 (2005).
[13] D. Comeau, A. Hache, and N. Melikechi, Appl. Phys. Lett. **83**, 246 (2003).
[14] D. S. Kliger, Acc. Chem. Res. **13**, 129 (1980).
[15] O. C. Mullins, E. Y. Sheu, A. Hammami, and A. G. Marshall, *Asphaltenes, Heavy Oils, and Petroleomics* (Springer, New York, 2006).
[16] G. Andreatta, C. G. Goncalves, G. Buffin, N. Bostrom, C. M. Quintella, F. Arteaga-Larios, E. Pérez, and O. C. Mullins, Energy Fuels **19**, 1282 (2005).
[17] S. Acevedo, B. Méndez, A. Rojas, H. Rivas, and I. Layrisse, Fuel **64**, 1741 (1985).
[18] S. Acevedo, M. A. Ranaudo, J. C. Pereira, J. Castillo, A. Fernandez, P. Pérez, and M. Caetano, Fuel **78**, 997 (1999).